ELSEVIER

Biophysical Chemistry 129 (2007) 163 – 171

Biophysical Chemistry

http://www.elsevier.com/locate/biophyschem

Interaction of myoglobin with poly(methacrylic acid) at different pH in their layer-by-layer assembly films: An electrochemical study

Wei Guo, Naifei Hu *

Department of Chemistry, Beijing Normal University, Beijing 100875, China

Received 29 March 2007; received in revised form 24 May 2007; accepted 25 May 2007
Available online 31 May 2007

Abstract

Myoglobin (Mb), with net positive surface charges at pH 5.0, was successfully assembled into layer-by-layer films on various solid surfaces with poly(methacrylic acid) (PMAA) at different pH, designated as $\{PMAA(pH\ 5.0)/Mb\}_n$, $\{PMAA(pH\ 6.5)/Mb\}_n$, and $\{PMAA(pH\ 8.0)/Mb\}_n$, respectively. As a weak polycarboxylic acid with $pK_a = 6$ - 7, PMAA carried different negative charges at different pH due to different ionization degree of its carboxylic acid groups. Quartz crystal microbalance (QCM), UV-vis spectroscopy, and cyclic voltammetry (CV) were used to monitor and confirm the assembly of $\{PMAA/Mb\}_n$ films. All the results showed that the adsorption amount of Mb in each bilayer had an "unexpected" sequence of $\{PMAA(pH\ 5.0)/Mb\}_n > \{PMAA(pH\ 6.5)/Mb\}_n > \{PMAA(pH\ 8.0)/Mb\}_n$, which could be explained by the formation of soluble complex of PMAA-Mb at pH 8.0 and the cooperative effect of hydrogen bonding and induced electrostatic interaction between Mb and PMAA at pH 5.0. The influence of ionic strength in exposure solution and in Mb adsorbate solution was investigated, and the results supported the above explanations. The $\{PMAA/Mb\}_n$ films provided a suitable microenvironment for Mb to retain its near-native structure and transfer electron with underlying electrodes. The reversible CV peak pair for Mb Fe(III)/Fe(II) redox couple could be used to catalyze reduction of hydrogen peroxide electrochemically, showing the potential applicability of the films as the new type of biosensors or bioreactors based on the direct electrochemistry of Mb. The electrochemical and electrocatalytic behaviors of protein layer-by-layer films with weak polyelectrolytes could thus be controlled by adjusting the solution pH of weak polyelectrolytes.

Keywords: Layer-by-layer assembly; Myoglobin; Poly(methacrylic acid); Direct electrochemistry; Interaction study

1. Introduction

Study of immobilization of enzymes and proteins is of great significance in bio-related sciences and technologies such as biosensors and biocatalysis [1,2]. There are numerous enzyme immobilization approaches including physical entrapment, surface adsorption, sol-gel encapsulation, covalent bonding, and others [3–7]. Among them, the layer-by-layer assembly technique, introduced by Decher in 1991 [8,9], is of particular interest. The layer-by-layer assembly was first developed for fabricating ultrathin films on solid surfaces by alternate adsorption of oppositely charged polyelectrolytes from their solutions, and then extended to build up films with other species including proteins [9,10]. Compared with cast and dip-coating methods, the layer-by-layer protocol allows the precise control of the film thickness at molecular or nanometer level with predesigned film composition and architecture. Over other molecular architecture methods such as Langmuir-Blodgett membrane and self-assembly monolayers (SAMs), the layer-by-layer assembly demonstrates distinguished advantages in its easiness in film preparation, no need of specific instrument, and the diversity of the types of adsorbed species and underlying solid substrates [9–11]. Proteins can be considered as a kind of natural polyelectrolytes and usually carry considerable net surface charges under suitable pH conditions. Thus, oppositely charged proteins and polyelectrolytes can be assembled into layer-by-layer films by electrostatic interaction between them. For instance, Lvov et al assembled multilayer films of positively charged myoglobin (Mb) and cytochrome $P450_{cam}$ (Cyt P450) with negatively charged DNA and polystyrenesulfonate (PSS) on gold electrodes [12]. Oppositely charged poly(diallyldimethylammonium) (PDDA)

* Corresponding author. Tel.: +86 10 5880 5498; fax: +86 10 5880 2075.
E-mail address: hunaifei@bnu.edu.cn (N. Hu).

0301-4622/$ - see front matter © 2007 Elsevier B.V. All rights reserved.
doi:10.1016/j.bpc.2007.05.015

and hemoglobin (Hb) were also successfully assembled into $\{PDDA/Hb\}_n$ layer-by-layer films on pyrolytic graphite (PG) electrodes by our group [13]. The direct electrochemistry of Mb, Cyt P450, and Hb at these layer-by-layer film electrodes was realized.

The development of protein layer-by-layer assembly requires the profound understanding of the essence of interaction between proteins and polyelectrolytes. The main driving force for the assembly is usually electrostatic interaction between oppositely charged substances [9], and the polyelectrolytes used for assembly of protein multilayer films are generally strong polyelectrolytes (that is, under conditions where the polyelectrolytes are essentially fully dissociated). However, when weak polyelectrolytes are involved, the interaction may become more complicated since the charge density and ionization of the weak polyelectrolytes varies with environmental pH. The study of interaction between proteins and weak polyelectrolytes in their layer-by-layer assembly has been seldom reported up to now [14], while the driving forces in the assembly of $\{polycation/polyanion\}_n$ multilayer films involving weak polyelectrolytes have been studied extensively [15–18]. For example, Sukhishvili et al studied the pH-dependent stabilization of layer-by-layer films composed of weak polycarboxylic acids and highly charged polycations [19]. The good stability of the films at lower pH was explained by the onset of hydrogen bonding involving protonated carboxylic acid groups within the films. Moreover, the increased local ionization of weak polycarboxylic acid in the presence of a highly charged polycation in their layer-by-layer films, compared to its ionization in solution, was reported [20,21]. This induced electrostatic interaction might also play an important role in the assembly of multilayer films involving weak polyelectrolytes at relatively low pH.

Poly(methacrylic acid) (PMAA) is a weak polyacid with pK_a at 6 - 7 [14]. PMAA has been used as a representative of weak polyelectrolytes in preparation of layer-by-layer films with highly charged polycations, and the driving forces and interaction between the building blocks have been studied [20–23]. Particularly, Sukhishvili et al investigated the assembly of layer-by-layer films of PMAA with positively charged proteins such as lysozyme, ribonuclease, and globulin, and studied their interaction and film stability under different pH and ionic strength conditions by in situ ATR-FTIR [14]. They found that the interaction between PMAA and proteins was not just simple electrostatic interaction and highly dependent on the assembly pH.

In the present work, Mb was selected as a model protein to study its interaction with weak polyacid PMAA at different pH in their layer-by-layer films. Mb showed nearly reversible electrochemical response in its layer-by-layer films with strong polyelectrolytes assembled on electrode surface [24,25]. We thus expected that the direct electrochemistry of Mb could also be realized in its multilayer films with the weak polyelectrolyte PMAA. The study of direct electrochemistry of redox proteins can be employed as a model in the mechanistic study of electron exchange among enzymes in biological systems, and can serve as a foundation for fabricating electrochemical biosensors and bioreactors without using chemical mediators [26,27]. Since the ionization of PMAA was different at different pH, the assembly behavior and the electrochemical response of $\{PMAA/Mb\}_n$ films assembled at various pH in PMAA adsorbate solution would be different. In this work, the assembly of $\{PMAA/Mb\}_n$ films was first realized and confirmed by quartz crystal microbalance (QCM), UV-vis absorption spectroscopy, and cyclic voltammetry (CV). The electrochemical and electrocatalytic properties of Mb in the films were then characterized. The interaction of positively charged Mb at pH 5.0 and PMAA at different pH was explored and discussed in detail. This work presents a new example of the interaction study between proteins and weak polyelectrolytes under different pH conditions, which may provide a possibility to control the ionization of weak polyelectrolyte by adjusting pH and then tune the adsorption amount of proteins in their layer-by-layer films. Since Mb is electroactive, different from those proteins used in the previous work [14], the present study may also provide a novel avenue to tailor the electrochemical and electrocatalytic behaviors of redox enzymes immobilized on electrode surface in biosensing and other biotechnological application.

2. Experimental

2.1. Chemicals

Poly(methacrylic acid, sodium salt) (PMAA, MW 75,100) was purchased from Fluka. Horse heart myoglobin (Mb, MW 17,800) was purchased from Sigma and used as received without further purification. Poly(diallyldimethylammonium) (PDDA, 20 wt %) and 3-mercapto-1-propanesulfonate (MPS, 90%) were from Aldrich. All other chemicals were reagent grade. Buffers were 0.01 M sodium acetate, sodium dihydrogen phosphate, boric acid, or citric acid, all containing 0.01 M NaCl. Buffer pH was adjusted with dilute HCl or KOH solutions. Twice-distilled water was used to prepare solutions.

2.2. Assembly of layer-by-layer films

For electrochemical study, basal plane pyrolytic graphite (PG, Advanced Ceramics, geometric area 0.16 cm^2) disk electrodes were polished on a metallographic sandpaper (280 grit) while being flushed with water. The electrodes were then ultrasonicated in water for 30 s and dried in air. A precursor layer of positively charged PDDA was adsorbed by immersing the PG electrodes into PDDA solutions (3 mg mL^{-1}) for 20 min. The PG/PDDA electrodes were then alternately immersed for 20 min in PMAA solutions (1 mg mL^{-1}, at pH 5.0, 6.5, or 8.0) and Mb solutions (1 mg mL^{-1}, at pH 5.0) with intermediate water washing and nitrogen stream drying. This cycle was repeated to obtain the desired number of bilayers (n), and the obtained layer-by-layer films are designated as $\{PMAA(pH\ 5.0)/Mb\}_n$, $\{PMAA(pH\ 6.5)/Mb\}_n$, and $\{PMAA(pH\ 8.0)/Mb\}_n$, respectively.

For UV-vis spectroscopic study, a quartz slide (0.8 × 4 cm, 1 mm thick) was immersed in a freshly prepared "piranha" solution (3:7 volume ratio of 30% H_2O_2 and 98% H_2SO_4. Caution: the piranha solution is highly corrosive and should be handled with extreme care. Only a small volume should be prepared at any time) for 30 min, rinsed carefully with water,

and then dried by nitrogen stream. The PDDA/{PMAA/Mb}$_n$ films were then assembled with the same procedure as on PG electrodes.

For quartz crystal microbalance (QCM) study, the gold QCM resonator electrodes were cleaned by depositing a few drops of piranha solution on the Au surface for 10 min. After being washed in water and pure ethanol successively, the gold QCM electrodes were immersed in MPS ethanol solution (4 mM) for 24 h to form an MPS monolayer and introduce negative charges on the gold surface. The precursor layer of PDDA and following {PMAA/Mb}$_n$ films were then assembled on the Au/MPS surface as on the PG electrodes. After each adsorption step, the electrodes were washed thoroughly in water, dried under nitrogen stream, and then the QCM frequency was measured in air. The sample films assembled on QCM gold electrodes were also used for microscopic Fourier transform infrared (FTIR) measurements.

2.3. Apparatus and procedures

A CHI 621B electrochemical workstation (CH Instruments) was used for CV, square wave voltammetry (SWV), and amperometry. A regular three-electrode cell was used with a saturated calomel electrode (SCE) as the reference electrode, a platinum wire as the counter electrode, and a PG disk with films as the working electrode. Buffers were purged with high-purity nitrogen for at least 15 min prior to electrochemical measurements. The nitrogen atmosphere was then maintained in the cell during the whole experiment.

QCM measurements were performed with a CHI 420 electrochemical analyzer (CH Instruments). The AT-cut quartz crystal resonators with fundamental frequency of 8 MHz coated with thin gold layers on both sides (surface area 0.196 cm^2) were used as electrodes. According to the Sauerbrey equation [28], the following formula was used to relate adsorbed mass, $\triangle$M (g), and frequency shift, $\triangle$F (Hz), by taking into account the properties of quartz resonator used in this work: $\triangle F = -7.40\times10^8\ \triangle M$. The nominal thickness of adsorbed layer, d (cm), can then be expressed as $d=(-6.8\times10^{-9})\ \triangle F/\rho$, where ρ is the density of the layer material (g cm^{-3}). For Mb, the density is about 1.3±0.1 g cm^{-3} [29].

UV-vis absorption spectroscopy was performed with a Cintra 10e spectrophotometer (GBC). FTIR spectra were obtained by using a NEXUS-670 FTIR spectrometer (Nicolet).

3. Results

3.1. Layer-by-layer assembly of {PMAA/Mb}$_n$ films

The layer-by-layer assembly of {PMAA/Mb}$_n$ films at different pH in PMAA adsorbate solution was monitored and confirmed by different techniques. QCM results showed that for all three {PMAA(pH 5.0)/Mb}$_n$, {PMAA(pH 6.5)/Mb}$_n$, and {PMAA(pH 8.0)/Mb}$_n$ films, a roughly linear frequency decrease with increase of the number of PMAA/Mb bilayers (n) was observed (Fig. 1), indicating the successful film assembly under different pH conditions. For a specific Mb film system, roughly constant -$\triangle$F value for each Mb adsorption layer

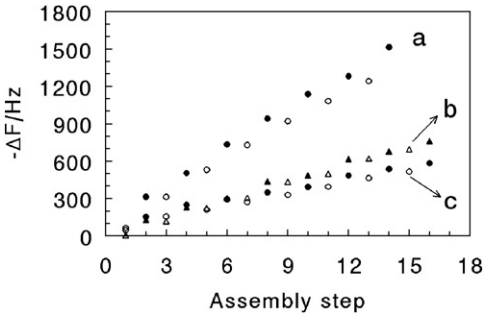

Fig. 1. QCM frequency shift with adsorption step for assembly of {PMAA/Mb}$_n$ films at different pH in PMAA adsorbate solution on Au/MPS/PDDA surface: (a) pH 5.0, (b) pH 6.5, and, (c) pH 8.0. The open marker represents PMAA adsorption step and the filled marker represents Mb adsorption step.

suggests that the amount of adsorbed Mb in each bilayer is approximately the same. However, in PMAA adsorption step, the frequency increase instead of decrease was observed in most cases, demonstrating the net decrease of mass. This was probably because of the partial desorption of previously adsorbed Mb out of the films when the films with Mb as the outermost layer was immerged into the PMAA solution. Nevertheless, the general trend of mass increase with n was observed in the whole assembly process and the overall growth of the films was not influenced by the partial desorption of Mb, indicating that PMAA was indeed adsorbed on the surface of Mb layer. Since the mass decrease caused by Mb desorption was larger than the mass increase caused by PMAA adsorption, the net mass decrease was observed in the PMAA adsorption step. For {PMAA(pH 5.0)/Mb}$_n$ films, the average decrease in frequency caused by the adsorption of Mb layer was 221±27 Hz, which would correspond to nominal thickness of 5.8 nm, roughly consistent with the dimension of Mb (2.5×3.5×4.5 nm^3 [30]), indicating the approximate monolayer adsorption of Mb. However, because of partial desorption of Mb in the PMAA adsorption step, the actual thickness of Mb layer in the films would become less than that of monolayer. While for {PMAA (pH 6.5)/Mb}$_n$ and {PMAA(pH 8.0)/Mb}$_n$ films, the average decrease in frequency caused by each adsorption layer of Mb was 102±14 and 82±14 Hz, and the corresponding thickness was 2.7 and 2.1 nm, respectively, all smaller than the average dimension of Mb. These results suggest that Mb molecules in its adsorption layer are loosely packed, and the three types of {PMAA/Mb}$_n$ films are arranged not in perfect order but with extensive interlayer mixing. The average frequency decrease for each Mb adsorption layer showed the sequence of {PMAA (pH 5.0)/Mb}$_n$ > {PMAA(pH 6.5)/Mb}$_n$ > {PMAA(pH 8.0)/Mb}$_n$.

Mb has a sensitive Soret absorption band for its heme group at about 408 nm, and UV-vis spectroscopy was used in this work to monitor the growth of {PMAA/Mb}$_n$ films on quartz slides modified by a PDDA precursor layer. Taking {PMAA(pH 5.0)/Mb}$_n$ as an example, the UV-vis spectra showed that the Soret band at 408 nm increased with the number of PMAA/Mb bilayers (n) (Fig. 2A). With the same n, the absorbance at 408 nm demonstrated the sequence of {PMAA(pH 5.0)/Mb}$_n$ > {PMAA (pH 6.5)/Mb}$_n$ > {PMAA(pH 8.0)/Mb}$_n$, and for all three types of {PMAA/Mb}$_n$ films, the absorbance had a linear relationship

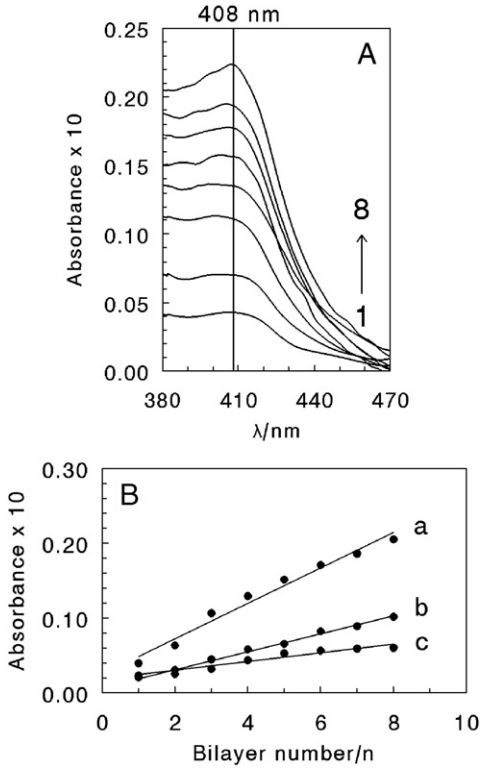

Fig. 2. (A) UV-vis spectra for $\{PMAA(pH\ 5.0)/Mb\}_n$ films with different numbers of bilayers (n). (B) Dependence of the absorbance at 408 nm on the number of bilayers (n) for $\{PMAA/Mb\}_n$ films assembled at different pH in PMAA solution: (a) pH 5.0, (b) pH 6.5, and (c) pH 8.0.

with n (Fig. 2B), in good agreement with the QCM results. These results confirm again that the growth of $\{PMAA/Mb\}_n$ films is roughly uniform, and the $\{PMAA(pH\ 5.0)/Mb\}_n$ films immobilize more amounts of Mb in each bilayer than those assembled at pH 6.5 or 8.0 in PMAA solution.

$\{PMAA/Mb\}_n$ films were also assembled on PG/PDDA electrodes and tested by CV. Taking $\{PMAA(pH\ 5.0)/Mb\}_n$ films as an example (Fig. 3A), the well-defined, nearly reversible reduction-oxidation CV peak pair at about -0.34 V vs SCE for Mb heme Fe(III)/Fe(II) redox couple [31] was used to monitor the growth of the films. The peak currents increased nonlinearly with the number of bilayers (n) up to 13. When $n > 13$, the peak currents essentially kept constant and did not increase anymore, indicating that Mb in the bilayers of $n > 13$ is no longer electroactive. If the number of bilayers at which the CV response began to reach the steady state was defined as n_{max}, the n_{max} would be equal to 13 for $\{PMAA(pH\ 5.0)/Mb\}_n$ films. The $\{PMAA(pH\ 6.5)/Mb\}_n$ and $\{PMAA(pH\ 8.0)/Mb\}_n$ films showed the same CV peak positions as the $\{PMAA(pH\ 5.0)/Mb\}_n$ films but the n_{max} was only about 10. In contrast, the PG/PDDA/PMAA films containing no Mb showed no CV response at all in the same potential window.

For a specific $\{PMAA/Mb\}_n$ film with a certain n value, CV showed symmetric peak shapes and nearly equal heights of their reduction and oxidation peaks, and the reduction peak currents increased linearly with scan rates from 0.05 to 2.0 V s^{-1}. These results are characteristics of diffusionless, surface-confined voltammetric behavior [32], indicating that all electroactive MbFe (III) in the films are converted to MbFe(II) on the forward cathodic scan, while on the reverse anodic scan, all MbFe(II) produced at electrodes are transformed back to MbFe(III). In this case, integration of CV reduction peak gives the charge (Q) value for full reduction of electroactive MbFe(III) in the films, which can be further converted to the surface concentration of electroactive Mb (Γ^*, mol cm^{-2}) in the films according to the Faraday's law [32]. All three types of $\{PMAA/Mb\}_n$ films displayed a nonlinear increase of Γ^* with n until 13 or 10, and afterwards the Γ^* values reached the steady state (Fig. 3B). With the same n, the Γ^* showed a sequence of $\{PMAA(pH\ 5.0)/Mb\}_n > \{PMAA(pH\ 6.5)/Mb\}_n > \{PMAA(pH\ 8.0)/Mb\}_n$, consistent with the results of QCM and UV-vis spectroscopy.

With the isoelectric point (pI) at 6.8 [33], Mb has net positive surface charges at pH 5.0. While as a weak polyacid, PMAA has its pK_a at 6 - 7 [14], and carries much more negative charges at pH 8.0 than at pH 5.0. Thus, the above sequence is difficult to explain by simple electrostatic interaction between Mb and PMAA, and the interaction must be complicated and will be discussed later in Discussion section.

3.2. Estimation of electrochemical parameters

SWV, as the pulse electrochemical approach [34], was used in this work to estimate the apparent heterogeneous electron transfer rate constant (k_s) and formal potential ($E^{o\prime}$) for $\{PMAA/Mb\}_{10}$ films with $n = 10$. As expected, three types of $\{PMAA/Mb\}_{10}$ films demonstrated well-defined SWV forward and reverse peaks for Mb Fe(III)/Fe(II) couple (not shown).

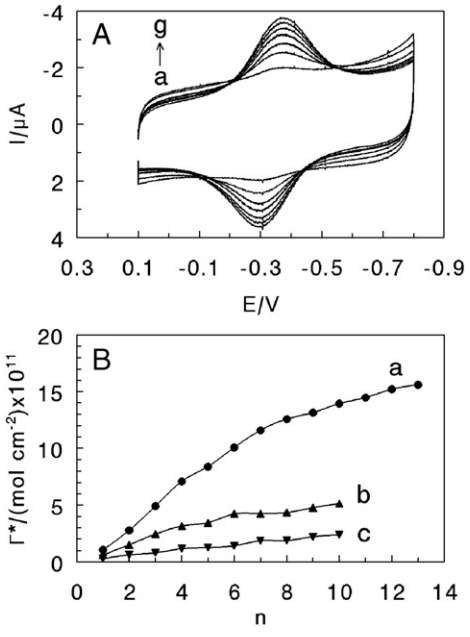

Fig. 3. (A) CVs at 0.2 V s^{-1} in pH 7.0 buffers for $\{PMAA(pH\ 5.0)/Mb\}_n$ films with the numbers of bilayers (n): (a) 1, (b) 3 (c) 5, (d) 7, (e) 9, (f) 11, (g) 13. (B) Dependence of surface concentration of electroactive Mb (Γ^*) on the number of bilayers (n) for $\{PMAA/Mb\}_n$ films assembled at different pH in PMAA solution: (a) pH 5.0, (b) pH 6.5, and (c) pH 8.0. Data are from CVs at 0.2 V s^{-1} in pH 7.0 buffers.

Nonlinear regression analysis was employed for SWV background-subtracted forward and reverse curves, using a model which combined the single-species surface-confined SWV model [35] and the formal potential dispersion model [36]. The detailed description of the nonlinear regression process was reported previously in the literatures [36,37]. The SWV data for $\{PMAA/Mb\}_{10}$ films showed goodness of fit onto the model over a range of amplitudes and frequencies. The average k_s values obtained from fitting SWV data at pH 7.0 for three kinds of Mb films were very close and relatively large (Table 1), which were qualitatively consistent with the quasi-reversible CV behaviors of the films. The other electrochemical parameters estimated by CV for the Mb films are also listed in Table 1 for comparison.

3.3. Effect of ionic strength

The influence of ionic strength in exposure solution on $\{PMAA(pH\ 5.0)/Mb\}_n$ and $\{PMAA(pH\ 8.0)/Mb\}_n$ films was first studied to investigate the character of interaction between Mb and PMAA at different pH.

The $\{PMAA/Mb\}_n$ films were immersed in pH 7.0 buffers with different ionic strength (or NaCl concentration, C_{NaCl}, in this study), CV was then carried out, and the surface concentration of electroactive Mb (Γ^*, mol cm^{-2}) in the films was estimated. In order to correct the electrode-to-electrode variation for the experiments, the relative adsorption amount or the ratio of Γ^*/Γ^{*0} instead of absolute surface concentration (Γ^*) was used in the comparison, where Γ^{*0} is defined as the surface concentration of electroactive Mb in the buffers containing 0.01 M NaCl (Fig. 4). For $\{PMAA(pH\ 8.0)/Mb\}_n$ films, the ratio of Γ^*/Γ^{*0} continuously decreased with increase of C_{NaCl}, while for $\{PMAA(pH\ 5.0)/Mb\}_n$ films, Γ^*/Γ^{*0} kept nearly constant at low NaCl concentration (<0.1 M), and then decreased with the ionic strength at higher C_{NaCl}.

To further investigate the property of interaction between Mb and PMAA at pH 5.0, the effect of ionic strength in Mb adsorbate solutions on the adsorption amount of Mb on PMAA surface was studied by both QCM and CV. In these studies, two PDDA/PMAA(pH 5.0) bilayers were firstly assembled on PG or Au/MPS surface as precursor layers to make the electrode surface more uniform and the following adsorption of Mb more reproducible from one preparation to another [38]. From the experimental results (Fig. 5), both Γ-C_{NaCl} curve measured by QCM and Γ^*-C_{NaCl} curve estimated by CV showed a similar peak-like shape and the same peak position. Γ and Γ^* values

Table 1
Electrochemical parameters of $\{PMAA/Mb\}_{10}$ films

films	Γ^*/ (mol cm^{-2})[a]	ΔE_p/ mV[a]	k_s/ s^{-1} [b]	E°′/V, vs SCE	
				CV[a]	SWV[b]
$\{PMAA(pH\ 5.0)/Mb\}_{10}$	1.39×10^{-10}	70	33±4	-0.342	-0.368
$\{PMAA(pH\ 6.5)/Mb\}_{10}$	0.51×10^{-10}	80	31±7	-0.347	-0.377
$\{PMAA(pH\ 8.0)/Mb\}_{10}$	0.21×10^{-10}	77	35±7	-0.345	-0.375

[a] Data are from CVs at 0.2 V s^{-1} in pH 7.0 buffers.
[b] Average values for analysis of ten SWVs at frequencies of 100 - 200 Hz, amplitudes of 60 and 75 mV, and step height of 4 mV, in pH 7.0 buffers.

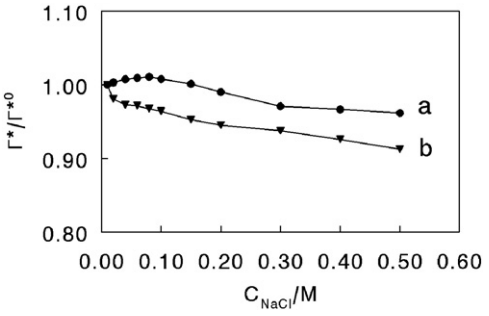

Fig. 4. Influence of NaCl concentration (C_{NaCl}) in pH 7.0 buffers on Γ^*/Γ^{*0} ratio for (a) $\{PMAA(pH\ 5.0)/Mb\}_8$ and (b) $\{PMAA(pH\ 8.0)/Mb\}_8$ films, where Γ^{*0} is the surface concentration of electroactive Mb in the buffers containing 0.01 M NaCl and Γ^* is the surface concentration of electroactive Mb in the buffers containing higher NaCl concentration. Γ^{*0} and Γ^* data are from CVs at 0.2 V s^{-1}.

increased with the ionic strength at low NaCl concentration and then decreased with the ionic strength at high C_{NaCl}, passing through a maximum point at 0.2 M. Under the same condition, Γ^* was always smaller than Γ. This is understandable since only parts of Mb in the films are electroactive.

3.4. Spectroscopic studies

The Soret absorption band of the heme prosthetic group may provide information on the secondary or tertiary structure of heme proteins, especially on the conformational change around the heme region [39,40]. The Soret band of dry $\{PMAA/Mb\}_8$ films assembled at different pH in PMAA adsorbate solution located at about 408 nm, very close to that of Mb in aqueous solution (409 nm), suggesting that Mb in three types of $\{PMAA/Mb\}_8$ films retains its near-native structure (Fig. 6A). The position of the Soret band depended on pH of external buffers. When $\{PMAA/Mb\}_8$ films were immersed into buffers at pH between 5.0 and 10.0, the Soret band was observed at 410 nm (Fig. 6B), very close to 409 nm for Mb in solution, and maintained a good peak shape. This suggests that Mb in $\{PMAA/Mb\}_8$ films essentially retains the original structure in the medium pH range. When pH was changed toward a more acidic direction, the peak shape became smaller and broader. At

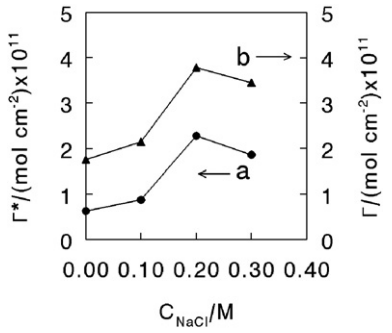

Fig. 5. Effect of NaCl concentration (C_{NaCl}) in Mb adsorbate solution on surface concentration of Mb adsorbed on surface of $\{PDDA/PMAA(pH\ 5.0)\}_2$ films. (a) Surface concentration of electroactive Mb (Γ^*) estimated by CV at 0.2 V s^{-1} in pH 7.0 buffers and (b) surface concentration of Mb (Γ) measured by QCM.

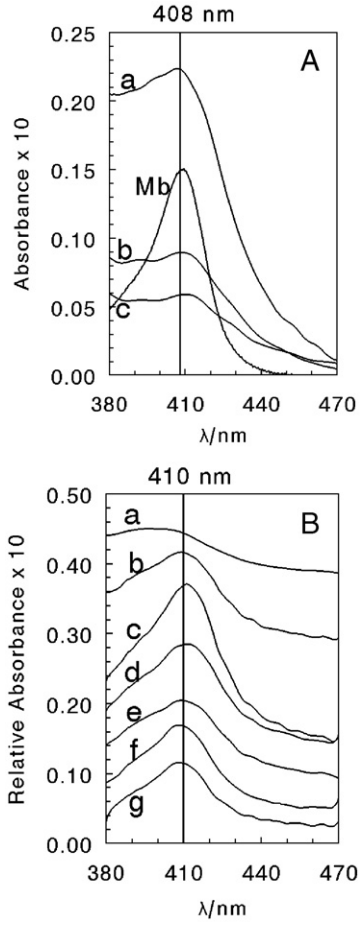

Fig. 6. (A) UV-vis spectra for dry $\{PMAA/Mb\}_8$ films assembled at different pH in PMAA solution: (a) pH 5.0, (b) pH 6.5, (c) pH 8.0, and the spectrum of Mb in pH 7.0 buffers. (B) UV-vis spectra of $\{PMAA(pH\ 5.0)/Mb\}_8$ films in buffers at (a) pH 4.0, (b) pH 5.0, (c) pH 7.0, (d) pH 9.0, and (e) pH 10.0. UV-vis spectra of (f) $\{PMAA(pH\ 6.5)/Mb\}_8$ and (g) $\{PMAA(pH\ 8.0)/Mb\}_8$ films in pH 7.0 buffers.

pH 4.0, for example, the Soret band of $\{PMAA(pH\ 5.0)/Mb\}_8$ films almost disappeared and showed a great blue-shift (Fig. 6B, curve a), indicating that Mb in $\{PMAA(pH\ 5.0)/Mb\}_8$ films may denature to a considerable extent in these relatively extreme pH environment.

It was reported that PMAA had two IR absorption peaks at around 1700 and 1554 cm^{-1}, respectively [14]. The former is attributed to the symmetric stretch vibrations of the uncharged form of carboxylic acid groups (-COOH), and the latter is ascribed to the asymmetric stretching vibration of the ionized carboxylate groups ($-COO^-$) of PMAA. From the relative IR intensity of these two peaks, the ionization degree of carboxylic acid groups of PMAA could be estimated [20,21]. The cast films of pure PMAA from its pH 5.0 solution showed a strong peak at about 1700 cm^{-1} and a relative weak peak at around 1554 cm^{-1} (Fig. 7, curve a), indicating that most of carboxylic acid groups of PMAA at pH 5.0 are not ionized. On the contrary, for the cast films of pure PMAA from its pH 8.0 solution, the peak of -COOH at 1700 cm^{-1} was much weaker than that of $-COO^-$ at 1554 cm^{-1} (Fig. 7, curve b), suggesting

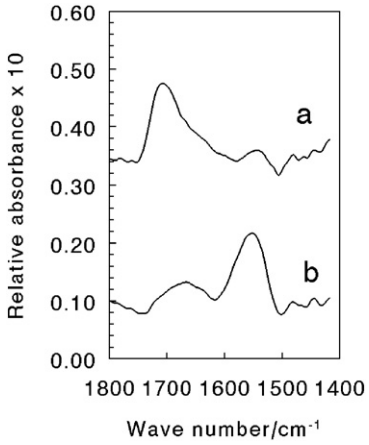

Fig. 7. FTIR spectra of cast PMAA films from (a) pH 5.0 and (b) pH 8.0 buffers.

the high degree of ionization of carboxylic acid groups of PMAA at this pH.

3.5. Electrocatalytic property of $\{PMAA(pH\ 5.0)/Mb\}_n$ films

Since the surface concentration of electroactive Mb (Γ*) of $\{PMAA(pH\ 5.0)/Mb\}_n$ films was much larger than that of $\{PMAA(pH\ 6.5)/Mb\}_n$ and $\{PMAA(pH\ 8.0)/Mb\}_n$ films (Fig. 3B and Table 1), $\{PMAA(pH\ 5.0)/Mb\}_n$ films were chosen as a representative of $\{PMAA/Mb\}_n$ films to investigate the electrocatalytic property of Mb in the films toward reduction of hydrogen peroxide.

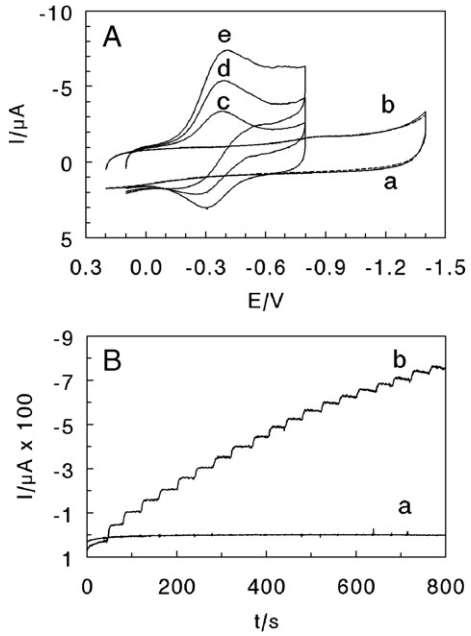

Fig. 8. (A) CVs at 0.2 V s^{-1} in pH 7.0 buffers for (a) PMAA films, (b) PMAA films with 55 μM H_2O_2 in solution, (c) $\{PMAA(pH\ 5.0)/Mb\}_{13}$ films, (d) $\{PMAA(pH\ 5.0)/Mb\}_{13}$ films with 25 μM H_2O_2, and (e) $\{PMAA(pH\ 5.0)/Mb\}_{13}$ films with 55 μM H_2O_2. (B) Amperometric current-time curves at constant potential of 0 V in pH 7.0 buffers with injection of H_2O_2 every 40 s for (a) PMAA and (b) $\{PMAA(pH\ 5.0)/Mb\}_{13}$ films with increment of 0.2 mM H_2O_2 at each step.

When H_2O_2 was added to pH 7.0 buffers, a significant increase in CV reduction peak at about -0.38 V for {PMAA(pH 5.0)/Mb}$_{13}$ films was observed with the decrease or even disappearance of the oxidation peak (Fig. 8A). However, direct reduction of H_2O_2 was not observed at blank PMAA film electrodes in the studied potential window. The catalytic reactivity of {PMAA(pH 5.0)/Mb}$_{13}$ films toward reduction of H_2O_2 was used to quantitatively determine the concentration of H_2O_2 in solution by CV. The linear relationship between electrocatalytic reduction peak current and H_2O_2 concentration was observed in the range of 1 – 50 μM. The calibration plot then tended to level off when the concentration of H_2O_2 became larger. When H_2O_2 concentration was larger than 68 μM, the catalytic peak current even decreased, suggesting a progressive enzyme inactivation in the presence of high concentration of reactant [41].

The electrocatalytic reduction of hydrogen peroxide at {PMAA(pH 5.0)/Mb}$_{13}$ film electrodes was also studied by amperometry. After optimization, the constant potential for amperometry was set at 0 V vs SCE for the Mb films, and the catalytic reduction current was monitored when aliquots of H_2O_2 were added (Fig. 8B). The stepped increase of H_2O_2 concentration in buffers resulted in the corresponding growth of reduction currents. In contrast, at protein-free PMAA film electrodes, no current response was observed after the addition of H_2O_2.

4. Discussion

The results of QCM, UV-vis spectroscopy, and CV experiments showed that Mb could be assembled into {PMAA/Mb}$_n$ layer-by-layer films with PMAA at different pH, and the adsorption amount of Mb in each bilayer demonstrated the sequence of {PMAA(pH 5.0)/Mb}$_n$ > {PMAA(pH 6.5)/Mb}$_n$ > {PMAA(pH 8.0)/Mb}$_n$ (Figs. 1–3). Considering that PMAA has pK_a at 6 - 7 [14] and carries much more negative charges at pH 8.0 than at pH 5.0 and Mb has net positive surface charges at pH 5.0, this sequence seems "counterintuitive" and is difficult to explain by simple electrostatic interaction between Mb and PMAA. The exploration of the interaction for different types of {PMAA/Mb}$_n$ films is discussed as follows.

For {PMAA(pH 8.0)/Mb}$_n$ films, while PMAA has the highest negative charge density as a result of ionization of its most carboxylic groups (Fig. 7), the adsorption amount of Mb in each bilayer is the smallest among the three types of {PMAA/Mb}$_n$ films (Figs. 1–3). This may be explained by the formation of soluble complex of PMAA-Mb. Izumrudov et al reported in the study of phase diagrams of mixed aqueous solutions of PMAA and positively charged proteins (lysozyme, chymotrypsinogene, or ribonuclease) that the soluble complexes of PMAA-protein would be formed under suitable conditions [42]. Sukhishvili et al found that the positively charged lysozyme was completely stripped off the surface of PMAA at pH higher than 7.0, and the growth of lysozyme/PMAA multilayer films was inhibited at pH > 7.0 [14]. This was interpreted by a large excess of negative charges introduced by PMAA, which was favorable for the formation of soluble PMAA-lysozyme complex. In the present work, the strong electrostatic interaction between oppositely charged Mb and PMAA at pH 8.0 under our experimental condition may also lead to the formation of PMAA-Mb complex that is soluble in solution, and then causes the less adsorption amount of Mb in the assembly of {PMAA(pH 8.0)/Mb}$_n$ films.

At pH 5.0, PMAA is essentially neutral and carries the smallest negative charges because most of the carboxylic acid groups are not ionized (Fig. 7). However, {PMAA(pH 5.0)/Mb}$_n$ films immobilize the largest amount of Mb among the three types of {PMAA/Mb}$_n$ films (Figs. 1–3). This may be explained by both hydrogen bonding and induced electrostatic interaction between Mb and PMAA. It was reported in the literature that the hydrogen bonding between protonated carboxylic acid groups (proton donors) of one polymer and amide groups (proton acceptor) of another polymer could be a predominant driving force for polymeric layer-by-layer assembly under certain circumstances [43–45]. For example, Rubner et al demonstrated that polymeric multilayers could be assembled through hydrogen bonding between polyacryamide and PMAA when the pH of the dipping and rinsing solutions of polymers was maintained below 4.0 [23]. Sukhishvili et al investigated the interaction between PMAA and some proteins (lysozyme, ribonuclease, or globulin) in their layer-by-layer films, and found that when the pH was set at relatively low value, the ionization of carboxylic acid groups in PMAA decreased drastically, and the hydrogen bonding would play an important role in the film assembly and stabilization [14]. In the present work, when pH = 5.0, the fraction of -COOH groups in PMAA is much larger than that of $-COO^-$ ones (Fig. 7), and Mb has many $-NH_2$ groups in their side chains of polypeptide backbones. Thus, the hydrogen bonding between -COOH groups of PMAA and $-NH_2$ groups of Mb would probably be one of the major driving forces for the assembly of {PMAA(pH 5.0)/Mb}$_n$ films. This speculation is further supported by the stability experiments of {PMAA/Mb}$_n$ films in buffers with different ionic strength (Fig. 4). The Γ^*/Γ^{*0} ratio decreases with C_{NaCl} monotonously for {PMAA(pH 8.0)/Mb}$_n$ films, indicating that the main interaction between PMAA and Mb is electrostatic interaction under this condition since the multilayer films constructed mainly by electrostatic interaction tend to be destroyed in solution of high ionic strength owing to screening effect [14,19]. While for {PMAA(pH 5.0)/Mb}$_n$ films, the Γ^*/Γ^{*0} ratio displays a different changing trend with C_{NaCl} (Fig. 4). The Γ^*/Γ^{*0} value keeps nearly constant at low NaCl concentration (<0.1 M), and then decreases with C_{NaCl} at higher ionic strength. This result suggests that at low C_{NaCl}, some non-electrostatic interaction such as hydrogen bonding predominates in the films since non-electrostatic interaction is not influenced by ionic strength.

On the other hand, induced electrostatic interaction between Mb and PMAA may also play an important role in the assembly of {PMAA(pH 5.0)/Mb}$_n$ films. It is reported that the ionization degree of weak polyacids depended on the local electrostatic environment, and the ionization of protonated PMAA at low pH could be induced by polycations or positively charged proteins in their multilayer films [14,19,20,46]. For example, Granick et al found that the ionization of the embedded PMAA oscillated with net charge of the top layer of multilayer films [47].

When the strong polycationic quaternized polyvinylpyridine (QPVP) was on the top, the ionization of PMAA would be induced and enhanced to a higher level than that of PMAA in bulk solution, while when the negatively charged PSS was on the top, the ionization of PMAA would be greatly limited and depressed to a lower level than that in PMAA solution. Sukhishvili et al observed that positively charged proteins such as lysozyme could effectively induce the ionization of protonated carboxylic acid groups of PMAA at low pH, and the induced electrostatic interaction between PMAA and proteins became one of the major driving forces in the assembly of their layer-by-layer films [47]. We thus speculate that during the layer-by-layer assembly of {PMAA(pH 5.0)/Mb}$_n$ films, the Mb at pH 5.0 would create a local environment with relatively high positive charges, and consequently induce the ionization of adjacent PMAA molecules. Therefore, the induced electrostatic interaction between Mb and PMAA also plays a major role in the construction of {PMAA(pH 5.0)/Mb}$_n$ films. This speculation is supported by the experiments of influence of ionic strength in Mb adsorbate solution on the adsorption amount of Mb on {PDDA/PMAA(pH 5.0)}$_2$ surface (Fig. 5). There were two contrary or opposite factors influencing the Γ or Γ* value. On the one hand, higher salt concentration would screen the electrostatic repulsion between individual Mb molecules with the same positive charges, which might lead to the more adsorption amount of Mb. On the other hand, higher ionic strength might weaken the electrostatic attraction between oppositely charged Mb and PMAA, which would result in the decrease of Mb adsorption. It could be therefore understandable that the peak-like curve was observed in the Γ (or Γ*) vs C_{NaCl} curve (Fig. 5), which usually comes out when two antagonistic forces govern a physical process [25,48]. These peak-like curves support the electrostatic character of the interaction between PMAA and Mb.

According to QCM results, the nominal thickness of PMAA (pH 5.0)/Mb bilayer is about 5.8 nm. The thickness of electroactive {PMAA(pH 5.0)/Mb}$_{13}$ films with n=13 would thus be about 75 nm. Considering the mixing or interpenetrating of neighboring layers in assembly and the estimation error, the actual thickness of {PMAA(pH 5.0)/Mb}$_{13}$ films might be less than this value. Nevertheless, the thickness of electroactive films should still be in the range of a few tens of nm. Similar situation would also happen for {PMAA(pH 6.5)/Mb}$_{10}$ and {PMAA(pH 8.0)/Mb}$_{10}$ films. It is impossible that Mb adsorbed in the outer layers would directly "tunnel" electrons to electrodes with such a long distance. It is also impossible that these Mb molecules would physically diffuse to the electrode surface through this distance in the film phase and then transfer electrons with electrodes in the time scale of CV scan. Therefore, it is most probable that the electron-transfer of Mb in the {PMAA/Mb}$_n$ films with underlying electrodes takes electron-hopping mechanism [49]. In electron hopping, neighboring Mb molecules in the film phase exchange electrons with each other, and the electron-transfer can thus be extend from electrode surface to Mb molecules inside the films through step-by-step hopping. According to Marcus theory [49], as long as the distance between two neighboring Mb molecules is small enough, the electron self-exchange could happen, and then could be extended to a quite long distance if the density of Mb in the films is high enough. In this case, the k_s estimated by SWV for the films (Table 1) reflects the overall heterogeneous electron transfer rate constant in the process.

5. Conclusion

Positively charged Mb at pH 5.0 and weak polyacid PMAA under different pH conditions are successfully assembled into {PMAA/Mb}$_n$ layer-by-layer films. The adsorption amount of Mb in each bilayer shows a sequence of {PMAA(pH 5.0)/Mb}$_n$ > {PMAA(pH 6.5)/Mb}$_n$ > {PMAA(pH 8.0)/Mb}$_n$, indicating that the interaction between Mb and PMAA is not just electrostatic but more complicated. For {PMAA (pH 8.0)/Mb}$_n$ films, while the main driving force of the assembly is electrostatic attraction between oppositely charged Mb and PMAA, the formation of soluble complex of Mb-PMAA may make the adsorption amount of Mb become smaller. For {PMAA (pH 5.0)/Mb}$_n$ films, while the ionization of PMAA is very limited at pH 5.0, the combination of hydrogen bonding and induced electrostatic interaction between Mb and PMAA may make the adsorption amount of Mb become much larger. The results indicate that the layer-by-layer films of proteins and weak polyelectrolytes at different pH may demonstrate distinct behavior and unique interaction character. The understanding of the essence of interactions between proteins and weak polyelectrolytes may be used to control the amount of proteins immobilized in the films via adjusting the pH values in the weak polyelectrolyte solutions. The advantages of layer-by-layer assembly, such as the precise control of film thickness at nanometer level and the simplicity in the assembly, combined with the controllable properties of weak polyelectrolytes like PMAA, may provide a novel approach for immobilization of enzymes or proteins. The {PMAA/Mb}$_n$ films also provide a favorable microenvironment for the protein, in which Mb retains its near-native structure, and the direct electron transfer of the protein with underlying electrodes is greatly enhanced. In addition, the direct electrochemistry of Mb in the {PMAA/Mb}$_n$ films can be applied to electrochemically catalyze some substrates such as hydrogen peroxide, which may establish a foundation for fabricating the new type of mediator-free biosensors. Through adjusting the pH and the ionization of weak polyelectrolytes, the adsorption amount of enzymes immobilized in the layer-by-layer films can be tailored, and the corresponding electrochemical and electrocatalytic responses can be controlled.

Acknowledgement

The financial support from the National Natural Science Foundation of China (20275006, 20475008) is acknowledged.

References

[1] G. Wilson, in: A. Turner, I. Karube, G. Wilson (Eds.), Biosensor, Oxford University Press, New York, 1987.
[2] M.F. Chaplin, C. Bucke (Eds.), Enzyme Technology, Cambridge University Press, Cambridge, U.K., 1990.

[3] M. Ozge, J.B. Christopher, Stable sensor layers self-assembled onto surfaces using azobenzene-containing polyelectrolytes, Analyst 126 (2001) 1861–1865.
[4] J. Rishpon, S. Gottesfeld, C. Campbell, Amperometric glucose sensors based on glucose oxidase immobilized in Nafion, Electroanalysis 6 (1994) 17–21.
[5] H. Gunasingham, C.B. Tan, Platinum-dispersed Nafion film modified glassy carbon as an electrocatalytic surface for an amperometric glucose enzyme electrode, Analyst 114 (1989) 695–698.
[6] D. Avnir, S. Braun, O. Lev, M. Ottolenghi, Enzymes and other proteins entrapped in sol-gel materials, Chem. Mater. 6 (1994) 1605–1614.
[7] R.A. Williams, H.W. Blanch, Covalent immobilization of protein monolayers for biosensor applications, Biosens. Bioelectron. 9 (1994) 159–167.
[8] G. Decher, J.D. Hong, Buildup of ultrathin multilayer films by a self-assembly process: I consecutive adsorption of anionic and cationic bipolar amphiphiles on charged surfaces, Macromol. Chem. Macromol. Symp. 46 (1991) 321–327.
[9] G. Decher, Fuzzy nanoassemblies: toward layered polymeric multicomposites, Science 277 (1997) 1232–1237.
[10] Y. Lvov, in: Y. Lvov, H. Mohwald (Eds.), Protein Architecture: Interfacing Molecular Assemblies and Immobilization Biotechnology, Marcel Dekker, New York, 2000, pp. 125–167.
[11] Y. Lvov, in: R.W. Nalwa (Ed.), Handbook of Surfaces and Interfaces of Materials, vol. 3, Academic Press, New York, 2001, pp. 170–189.
[12] Y. Lvov, Z. Lu, J.B. Schenkman, X. Zu, J.F. Rusling, Direct electrochemistry of myoglobin and cytochrome P450cam in alternate layer-by-layer films with DNA and other polyions, J. Am. Chem. Soc. 120 (1998) 4073–4080.
[13] P. He, N. Hu, G. Zhou, Assembly of electroactive layer-by-layer films of hemoglobin and polycationic poly(diallyldimethylammonium), Biomacromolecules 3 (2002) 139–146.
[14] V.A. Izumrudov, E. Kharlampieva, S.A. Sukhishvili, Multilayers of a globular protein and a weak polyacid: role of polyacid ionization in growth and decomposition in salt solutions, Biomacromolecules 6 (2005) 1782–1788.
[15] D. Kovacevic, S. van der Burgh, A. de Keizer, M.A.C. Stuart, Specific ionic effects on weak polyelectrolyte multilayer formation, J. Phys. Chem., B 107 (2003) 7998–8002.
[16] S.T. Dubas, J.B. Schlenoff, Polyelectrolyte multilayers containing a weak polyacid: construction and deconstruction, Macromolecules 34 (2001) 3736–3740.
[17] S.E. Burke, C.J. Barrett, pH-dependent loading and release behavior of small hydrophilic molecules in weak polyelectrolyte multilayer films, Macromolecules 37 (2004) 5375–5384.
[18] J. Choi, M.F. Rubner, Influence of the degree of ionization on weak polyelectrolyte multilayer assembly, Macromolecules 38 (2005) 116–124.
[19] V. Izumrudov, S.A. Sukhishvili, Ionization-controlled stability of polyelectrolyte multilayers in salt solutions, Langmuir 19 (2003) 5188–5191.
[20] E. Kharlampieva, S.A. Sukhishvili, Ionization and pH stability of multilayers formed by self-assembly of weak polyelectrolytes, Langmuir 19 (2003) 1235–1243.
[21] A.F. Xie, S. Granick, Local electrostatics within a polyelectrolyte multilayer with embedded weak polyelectrolyte, Macromolecules 35 (2002) 1805–1813.
[22] S.A. Sukhishvili, S. Granick, Layered, erasable polymer multilayers formed by hydrogen-bonded sequential self-assembly, Macromolecules 35 (2002) 301–310.
[23] S.Y. Yang, J.D. Mendelsohn, M.F. Rubner, New class of ultrathin, highly cell-adhesion-resistant polyelectrolyte multilayers with micropatterning capabilities, Biomacromolecules 4 (2003) 987–994.
[24] H. Ma, N. Hu, J.F. Rusling, Electroactive myoglobin films grown layer-by-layer with poly(styrenesulfonate) on pyrolytic graphite electrodes, Langmuir 16 (2000) 4969–4975.
[25] P. He, N. Hu, Interactions between heme proteins and dextran sulfate in layer-by-layer assembly films, J. Phys. Chem., B 108 (2004) 13144–13152.
[26] F.A. Armstrong, G.S. Wilson, Recent developments in Faradaic bioelectrochemistry, Electrochim. Acta 45 (2000) 2623–2645.
[27] J.F. Rusling, Enzyme bioelectrochemistry in cast biomembrane-like films, Acc. Chem. Res. 31 (1998) 363–369.
[28] G. Sauerbrey, Verwendung von schwingquarzen zur wagung dunner schichten und zur mikrowagung, Z. Phys. 155 (1959) 206–214.
[29] T.E. Creighton (Ed.), Protein Structure, A Practical Approach, IRL Press, New York, 1990, p. 43.
[30] J.C. Kendrew, D.C. Phillips, V.C. Shore, Structure of myoglobin: a three-dimensional Fourier synthesis at 2 Å resolution, Nature 185 (1960) 422–427.
[31] J.F. Rusling, A.-E.F. Nassar, Enhanced electron transfer for myoglobin in surfactant films on electrodes, J. Am. Chem. Soc. 115 (1993) 11891–11897.
[32] R.W. Murray, in: A.J. Bard (Ed.), Electroanalytical Chemistry, vol. 13, Marcel Dekker, New York, 1984, pp. 191–368.
[33] A. Bellelli, G. Antonini, M. Brunori, B.A. Springer, S.J. Sligar, Transient spectroscopy of the reaction of cyanide with ferrous myoglobin. Effect of distal side residues, J. Biol. Chem. 265 (1990) 18898–18901.
[34] J.G. Osteryoung, J.J. O'Dea, in: A.J. Bard (Ed.), Electroanalytical Chemistry, vol. 14, Marcel Dekker, New York, 1986, pp. 209–325.
[35] J.J. O'Dea, J.G. Osteryoung, Characterization of quasi-reversible surface processes by square-wave voltammetry, Anal. Chem. 65 (1993) 3090–3097.
[36] Z. Zhang, J.F. Rusling, Electron transfer between myoglobin and electrodes in thin films of phosphatidylcholines and dehexadecylphosphate, Biophys. Chem. 63 (1997) 133–146.
[37] A.-E.F. Nassar, Z. Zhang, N. Hu, J.F. Rusling, T.F. Kumosinski, Proton-coupled electron transfer from electrodes to myoglobin in ordered biomembrane-like films, J. Phys. Chem., B 101 (1997) 2224–2231.
[38] G. Ladam, P. Schaad, J.C. Voegel, P. Schaaf, G. Decher, F. Cuidinier, In situ determination of the structural properties of initially deposited polyelectrolyte multilayers, Langmuir 16 (2000) 1249–1255.
[39] H. Theorell, A. Ehrenberg, Spectrophotometric, magnetic, and titrimetric studies on the heme-linked groups in myoglobin, Acta Chem. Scand. 5 (1951) 823–848.
[40] P. George, G. Hanania, Spectrophotometric study of ionizations in methemoglobin, Biochem. J. 55 (1953) 236–243.
[41] S.A. Adeiran, A.M. Lambeir, Kinetics of the reaction of compound II of horseradish peroxidase with hydrogen peroxide to form compound III, Eur. J. Biochem. 186 (1989) 571–576.
[42] V.A. Izumrudov, S.H. Lim, Controlled phase separations in solutions of poly(methacrylate) anion complexes with globular proteins, Polym. Sci., Ser. A 44 (2002) 484–490.
[43] A. Asano, Hydrogen-bond interaction of PMAA/PVAc blends: a natural abundant two-dimensional exchange 13C NMR investigation, Polym. J. 36 (2004) 23–27.
[44] C. Huang, F. Chang, Comparison of hydrogen bonding interaction between PMMA/PMAA blends and PMMA-co-PMAA copolymers, Polymer 44 (2003) 2965–2974.
[45] E. Diez-Pena, I. Quijada-Garrido, J.M. Barrales-Rienda, Advanced ^{1}H solid-state NMR spectroscopy on hydrogels, Macromol. Chem. Phys. 205 (2004) 430–437.
[46] F. Boulmedais, M. Bozonnet, P. Schwinte, J.-C. Voegel, P. Schaaf, Multilayered polypeptide films: secondary structures and effect of various stresses, Langmuir 19 (2003) 9873–9882.
[47] A.F. Xie, S. Granick, Weak versus strong: a weak polyacid embedded within a multilayer of strong polyelectrolytes, J. Am. Chem. Soc. 123 (2001) 3175–3176.
[48] G. Ladam, C. Gergely, B. Senger, G. Decher, J.C. Voegel, P. Schaaf, F.J.G. Cuisiner, Protein interactions with polyelectrolyte multilayers: Interactions between human serum albumin and polystyrene sulfonate/polyallylamine multilayers, Biomacromolecules 1 (2000) 674–687.
[49] M. Majda, in: R.W. Murray (Ed.), Molecular Design of Electrode Surfaces, New York, Wiley, 1992, pp. 159–206.